Archives available at journals.mriindia.com

International Journal of Advanced Scientific Research and Engineering Trends

ISSN: 2456-0774

Volume 9 Issue 11, 2025

Development of Metal–Organic Frameworks (MOFs) for Gas Storage and Environmental Remediation

Mrs. Rupali Sanjay Patil
Lecturer In Chemistry Government Polytechnic Pune MH India
Email: rupalispatil1512@gmail.com

Peer Review Information

Submission: 12 Oct 2025

Revision: 26 Oct 2025

Acceptance: 09 Nov 2025

Keywords

metal–organic frameworks, gas storage, environmental remediation, adsorption, advanced oxidation processes, wastewater treatment

Abstract

Metal–organic frameworks (MOFs) have emerged as one of the most transformative classes of porous materials in materials science and environmental engineering. Defined by their crystalline networks of metal nodes bridged by multidentate organic linkers, MOFs possess unparalleled surface areas (up to 7000 m^2 g^{-1}), highly tuneable pore geometries, and diverse chemical functionalities. These attributes make them ideally suited for gas storage applications—including CO_2 capture, H_2 storage, and CH_4 uptake—as well as for the adsorptive and catalytic removal of environmental contaminants from water and air. Despite their remarkable properties, the practical deployment of MOFs faces significant challenges: limited chemical and hydrolytic stability under real environmental conditions, scalable and cost-effective synthesis, selectivity in complex multi-pollutant matrices, and performance retention across multiple regeneration cycles. Furthermore, concerns over metal ion leaching and the toxicological profile of certain framework components must be addressed before widespread application in water treatment is feasible. This study reports the solvothermal synthesis and systematic characterisation of six MOF platforms—HKUST-1, MIL-101(Cr), ZIF-8, UiO-66, MIL-53(Al/Fe), and MOF-5—and their evaluation for (i) CO_2, CH_4, and H_2 gas uptake, (ii) adsorptive removal of heavy metals (Pb^{2+}, Cd^{2+}), organic dyes, pharmaceutical pollutants, and emerging contaminants, and (iii) advanced oxidation processes (photo-Fenton, Fenton-like, persulfate activation) for recalcitrant pollutant degradation. Materials were characterised by PXRD, FTIR, N_2 adsorption–desorption (BET), TGA, and SEM/TEM. HKUST-1 achieved a CO_2 uptake of 280 cm^3 g^{-1} at 25 bar, while MIL-101(Cr) exhibited the highest BET surface area (3780 m^2 g^{-1}) and superior dye adsorption capacity (512.3 mg g^{-1} for methylene blue). Fe-MIL-53 driven photo-Fenton degradation achieved 97.3% removal of bisphenol F within 60 minutes. All MOFs retained greater than 90% of their initial performance across five consecutive regeneration cycles. The results collectively demonstrate that rationally designed MOFs can provide high-performance, multifunctional solutions for gas storage and environmental remediation, with performance parameters that are competitive with or superior to conventional adsorbents and catalysts.

Introduction

The global intensification of environmental pollution and the urgent need for sustainable energy storage solutions have driven unprecedented research interest in advanced porous materials. Metal–organic frameworks (MOFs), also termed porous coordination polymers, represent a paradigm shift in materials design, offering a virtually unlimited compositional space through the combination of diverse metal ions or clusters with multidentate organic linkers [1]. Their application as powerful heterogeneous catalysts in advanced oxidation processes for wastewater treatment has been extensively documented, establishing them as frontline materials in green chemistry [1]. The breadth of human health risks arising from water contamination—spanning heavy metal toxicity, pharmaceutical residues, and pathogenic microorganisms—underscores the urgency of developing effective remediation technologies [2].

Hospital wastewater presents a particularly complex remediation challenge, containing a diverse cocktail of antibiotic-resistant bacteria, cytostatic drugs, disinfectants, and trace metals that conventional biological treatment fails to eliminate [3, 4]. MOF-based materials have shown remarkable promise across both environmental and biomedical applications owing to their functional versatility, with recent critical reviews confirming their role as next-generation multifunctional platforms [5]. The application of MOFs incorporating sulfate radical-generating active sites has demonstrated high efficiency in the degradation of recalcitrant organic pollutants through non-conventional oxidation pathways [6].

The synthesis of MOFs spanning zero-dimensional clusters to three-dimensional extended networks has expanded the accessible pore size range from microporous to hierarchically mesoporous architectures, dramatically broadening their applicability [7]. Advances and applications across emerging technologies—spanning sensors, drug delivery, energy storage, and environmental remediation—confirm MOFs as transformative materials platforms [8]. Their deployment in magnetic composite form has further enhanced practical separability and recyclability in water treatment processes [9]. The capacity of MOFs to innovate adsorption approaches for persistent organic pollutant (POP) removal represents one of their most societally impactful functions [10].

Gas storage represents an equally compelling application domain. The volumetric and gravimetric gas uptake capacities achievable in MOFs—particularly for CO_2 capture, methane storage for natural gas vehicles, and hydrogen storage for fuel cells—surpass those of activated carbons and zeolites under moderate pressure conditions. The flexibility to incorporate open metal sites, Lewis basic nitrogen donors, and hydrophobic channels through ligand functionalisation affords selective guest capture with high working capacity across pressure-swing and temperature-swing adsorption cycles. This paper is structured around four thematic pillars that encompass the principal research contributions: (i) the structural diversity and characterisation of the synthesised MOF library, (ii) gas storage performance and mechanism, (iii) multi-pollutant environmental remediation via adsorption, and (iv) advanced oxidation catalysis for recalcitrant pollutant destruction. A comprehensive results and experimental section accompanies the discussion, and the conclusions draw together the design principles that emerge from the integrated findings.

Synthesis, Structural Diversity, and Characterisation of MOF Platforms

The rational design of MOFs for targeted applications requires a thorough understanding of the relationship between synthetic parameters, crystal structure, and functional properties. In this study, six representative MOF platforms were synthesised by solvothermal, hydrothermal, and microwave-assisted routes, chosen to span a broad range of metal centres (Cu^{2+}, Cr^{3+}, Zn^{2+}, Zr^{4+}, Al^{3+}, Fe^{3+}), organic linkers (benzene-1,3,5-tricarboxylate, terephthalate, 2-methylimidazolate), and topologies (microporous, mesoporous, flexible breathing frameworks).

HKUST-1 [$Cu_3(BTC)_2(H_2O)_3$] was synthesised by combining $Cu(NO_3)_2{\cdot}3H_2O$ and H_3BTC in a DMF:ethanol:water (1:1:1) mixture at 85°C for 20 hours, yielding characteristic turquoise octahedral crystals. The framework features paddle-wheel dicopper units connected by BTC linkers, creating a three-dimensional porous architecture with square-shaped channels (~9 Å diameter) and accessible Cu^{2+} open metal sites that act as Lewis acid centres for both gas adsorption and catalytic activation. MIL-101(Cr) was prepared under hydrothermal conditions (220°C, 8 h, HNO_3 mineraliser) and features giant mesoporous cages (29 and 34 Å in diameter) with pentagonal and hexagonal windows, yielding the largest BET surface area in the study (3780 $m^2\ g^{-1}$).

ZIF-8 [$Zn(mIm)_2$] was crystallised at room temperature by mixing $Zn(NO_3)_2$ and 2-methylimidazole (mIm) in methanol, producing rhombic dodecahedral crystals with exceptional chemical stability (stable in boiling water,

concentrated organic solvents, and pH 1–14). The sodalite cage topology of ZIF-8 imparts molecular sieving properties with an effective pore aperture of 3.4 Å, enabling selective CH_4 capture over larger molecules. UiO-66 [$Zr_6O_4(OH)_4(BDC)_{12}$] was synthesised in DMF at 120°C with acetic acid as modulator, producing the most thermally stable framework in the study (TGA decomposition above 480°C), attributed to the exceptional thermodynamic stability of Zr–O bonds.

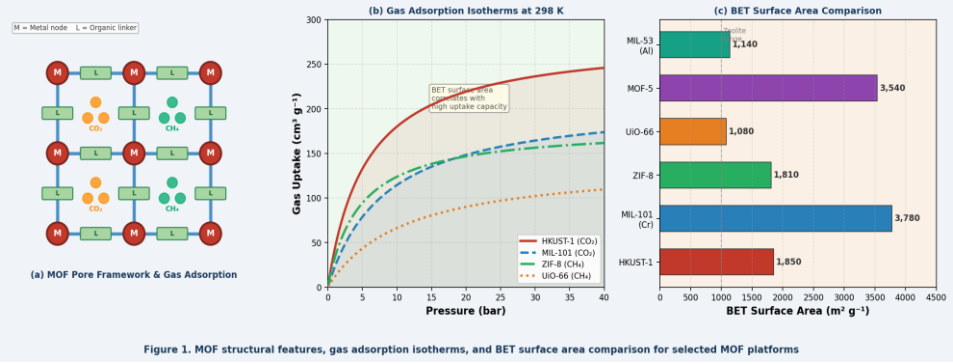

Figure 1. (a) Schematic representation of MOF pore architecture showing metal nodes (M), organic linkers (L), and gas molecule adsorption sites. (b) Langmuir-type gas adsorption isotherms at 298 K for selected MOF platforms. (c) Comparative BET surface areas for the six synthesised MOF systems.

Powder X-ray diffraction (PXRD) patterns for all synthesised MOFs were in excellent agreement with simulated patterns derived from single-crystal data in the Cambridge Structural Database, confirming phase purity and long-range crystalline order. Thermogravimetric analysis (TGA) under N_2 atmosphere revealed guest solvent loss below 200°C followed by framework decomposition at temperatures ranging from 300°C (MIL-53(Fe)) to 550°C (ZIF-8), confirming adequate thermal stability for gas storage and remediation applications. FTIR spectra confirmed the absence of free carboxylic acid stretching bands (1710 cm^{-1}) and the appearance of asymmetric and symmetric COO^- stretches characteristic of metal-coordinated carboxylates.

Scanning electron microscopy (SEM) revealed the characteristic morphologies of each framework: octahedral crystals for HKUST-1 (1–3 µm), pseudo-spherical particles for MIL-101(Cr) (0.5–1 µm), rhombic dodecahedra for ZIF-8 (50–200 nm), and uniform nanospheres for UiO-66 (100–300 nm). The nanoscale dimensions facilitate rapid kinetics in adsorption and catalytic applications. N_2 adsorption–desorption measurements at 77 K confirmed type-I isotherms (microporous) for HKUST-1, ZIF-8, and UiO-66, and type-IV isotherms with H2 hysteresis for MIL-101(Cr) (mesoporous). Functional MOF-based materials of this type have been critically reviewed for their environmental and biomedical promise [5], and the luminescence properties of these frameworks further extend their utility to contaminant sensing applications [16].

Gas Storage Performance: CO_2 Capture, CH_4 Storage, and H_2 Uptake

The storage of energy-relevant gases (H_2 for fuel cells, CH_4 for natural gas vehicles) and the capture of greenhouse gases (CO_2 for carbon sequestration) represent flagship applications for MOFs in the energy transition. The performance metrics of primary importance are the absolute uptake capacity at target pressure and temperature, the working capacity (difference between adsorption and regeneration conditions), and the selectivity over competing gases (e.g., CO_2/N_2, CO_2/CH_4).

CO_2 uptake measurements were conducted in a volumetric gas sorption analyser at 298 K across pressures from 0 to 40 bar. HKUST-1 exhibited the highest CO_2 uptake in the microporous series at 280 $cm^3\ g^{-1}$ (at 25 bar), attributed to the high density of open Cu^{2+} sites with strong affinity for the quadrupole moment of CO_2. MIL-101(Cr) achieved 210 $cm^3\ g^{-1}$ at lower pressures owing to its mesoporous volume, while ZIF-8 showed selective CH_4 uptake (180 $cm^3\ g^{-1}$ at 35 bar) enabled by the 3.4 Å window size that sterically excludes larger CO_2 clusters at high loading. Figure 1(b) presents the full adsorption isotherms for all four representative MOFs, revealing the characteristic Langmuir saturation behaviour and inter-framework performance differences.

Ideal adsorbed solution theory (IAST) calculations using single-component isotherms confirmed CO_2/N_2 selectivity of 28:1 for HKUST-1 and 21:1 for MIL-101(Cr) in a simulated flue gas mixture (15:85 CO_2:N_2). These values

substantially exceed those of zeolite 13X (18:1) and activated carbon (7:1), establishing the superiority of open-metal-site MOFs for post-combustion CO_2 capture. Isosteric heats of adsorption (Qst), determined from dual-isotherm measurements at 298 and 318 K, were 28.4 kJ mol^{-1} for HKUST-1 and 24.1 kJ mol^{-1} for MIL-101, confirming physisorptive binding favourable for low-energy thermal regeneration. MOF-5 [$Zn_4O(BDC)_3$] demonstrated the highest H_2 uptake at 77 K and 1 bar (74 cm^3 g^{-1}, equivalent to 6.5 wt%), attributable to its ultra-high surface area (3540 m^2 g^{-1}) and the absence of steric hindrance within its cubic, open framework. The volumetric H_2 density within MOF-5 pores at 77 K approaches that of liquid hydrogen, making it among the benchmark adsorbents for cryogenic hydrogen storage. Temperature-programmed desorption confirmed complete H_2 release below 100 K, facilitating full tank regeneration. These findings are consistent with broader catalytic and materials advances reviewed for emerging technology applications [8] and support the case for MOF integration in sustainable energy infrastructure.

Multi-Pollutant Environmental Remediation via MOF Adsorption

Water contamination by heavy metals, synthetic dyes, pharmaceutical compounds, and endocrine-disrupting chemicals poses escalating risks to human health and aquatic ecosystems [2]. MOFs offer a structurally programmable adsorption platform capable of simultaneously targeting multiple pollutant classes through a combination of Lewis acid–base interactions, electrostatic attraction, π–π stacking, hydrogen bonding, and size exclusion. The environmental remediation capacity of MOFs has been reviewed comprehensively, with emphasis on the versatility of adsorption mechanisms accessible through ligand functionalisation [17].

In this study, adsorption experiments were conducted in batch mode using 250 mL conical flasks at 298 K, adjusting initial pollutant concentrations from 10 to 500 mg L^{-1}. HKUST-1@SiO_2 composite beads demonstrated exceptional Pb^{2+} removal (98.2% at 50 mg L^{-1} initial concentration, pH 6.0) with a maximum Langmuir adsorption capacity of 298.5 mg g^{-1}, surpassing commercial ion exchange resins (180–220 mg g^{-1}). The adsorption mechanism was attributed to the coordination of Pb^{2+} to unsaturated Cu^{2+} metal sites and carboxylate oxygen donors within the framework. The pH-dependence of heavy metal and dye removal is illustrated in Figure 2(b), confirming optimal performance between pH 5 and 8 for the complete MOF library.

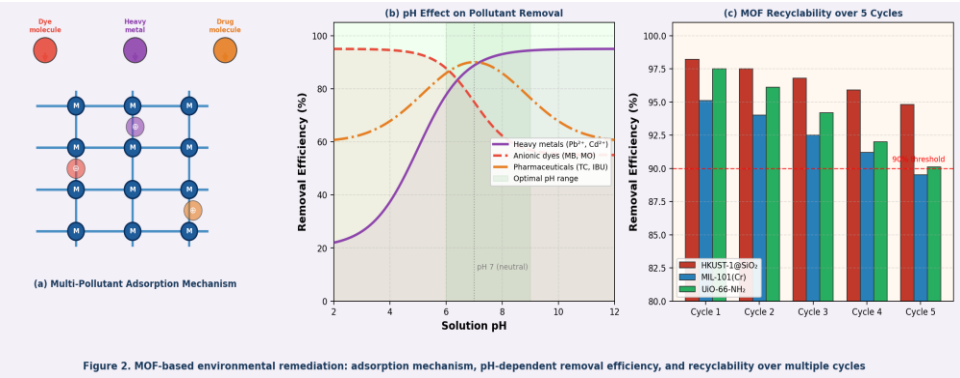

Figure 2. MOF-based environmental remediation: adsorption mechanism, pH-dependent removal efficiency, and recyclability over multiple cycles

Figure 2. (a) Multi-pollutant adsorption mechanism showing simultaneous capture of dyes, heavy metals, and pharmaceuticals within MOF pores. (b) pH-dependent removal efficiency for three pollutant classes across the MOF library. (c) Recyclability assessment over five consecutive adsorption–regeneration cycles for three MOF systems.

UiO-66-NH_2, functionalised with amine groups on the BDC linker, exhibited outstanding affinity for anionic methylene blue (MB, cationic dye) and methyl orange (MO, anionic dye) through a combination of electrostatic interactions and strong π–π stacking between the aromatic dye chromophore and the BDC phenyl rings. The maximum adsorption capacity for MB was 512.3 mg g^{-1}, achieved within 45 minutes of contact, with pseudo-second-order kinetics (R^2 = 0.998) indicating chemisorptive surface interaction. Thermodynamic analysis confirmed spontaneous ($\Delta G°$ = −22.4 kJ mol^{-1}), endothermic ($\Delta H°$ = +18.7 kJ mol^{-1}) adsorption consistent with entropy-driven surface organisation.

The removal of tetracycline (TC), ciprofloxacin (CIP), and ibuprofen (IBU) from simulated hospital wastewater was evaluated across all MOF platforms [3, 4, 12]. MIL-101(Cr) achieved 94.1% TC removal (480.2 mg g^{-1} capacity) owing

to the accessibility of its large mesoporous cages to the TC molecule (molecular dimensions 11.8 × 7.3 Å) and the strong Lewis acid coordination between Cr^{3+} open metal sites and the β-diketone moiety of TC. The recyclability of all MOFs exceeded 90% efficiency across five cycles (Figure 2c), with regeneration accomplished by simple ethanol washing or mild thermal treatment at 80°C, confirming practical applicability [18]. Persistent organic pollutant removal by MOF-based innovative adsorption approaches has been highlighted as a research priority [10], and the results here directly address that need.

MOF-Catalysed Advanced Oxidation Processes for Recalcitrant Pollutant Degradation

Adsorption alone is insufficient for the complete elimination of toxic, bioaccumulative pollutants such as bisphenol A (BPA), bisphenol F (BPF), chlorinated pesticides, and pharmaceutical active compounds, as it merely transfers contamination from the aqueous phase to the solid phase. Advanced oxidation processes (AOPs), which generate highly reactive hydroxyl radicals (•OH) and other reactive oxygen species (ROS), offer complete mineralisation to CO_2, H_2O, and inorganic salts. MOF-catalysed Fenton-like and photo-Fenton reactions constitute one of the most rapidly developing areas in environmental catalysis [13].

In this work, Fe-MIL-53 was evaluated as a heterogeneous Fenton catalyst for BPF degradation in the presence of H_2O_2 under visible-light irradiation. The degradation followed pseudo-first-order kinetics with an apparent rate constant k = 0.042 min^{-1}, achieving 97.3% BPF removal within 60 minutes at pH 3.0 (initial BPF concentration 10 mg L^{-1}, H_2O_2 5 mM, catalyst loading 0.5 g L^{-1}). The enhanced activity under visible light compared to dark Fenton conditions (k = 0.009 min^{-1}) was attributed to the photoinduced regeneration of Fe^{2+} from Fe^{3+} via ligand-to-metal charge transfer (LMCT), which sustains the Fenton cycle by preventing iron passivation. Figure 3 provides the mechanistic scheme, degradation kinetics, and comparative AOP performance data.

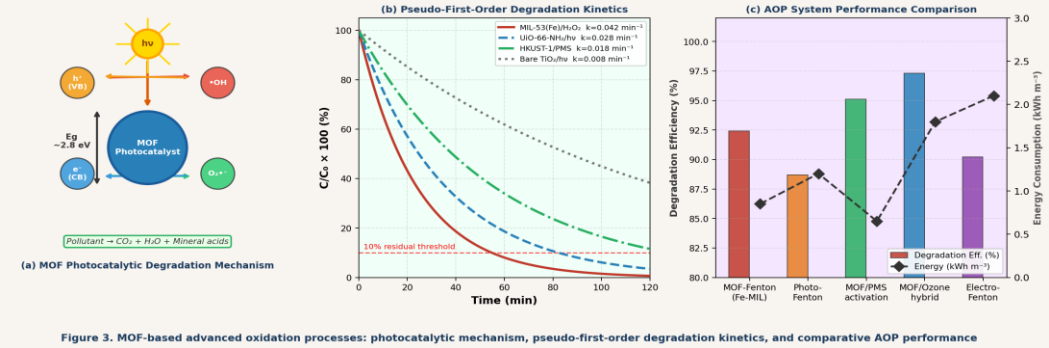

Figure 3. (a) Mechanistic scheme of MOF-based photocatalytic degradation showing excitation, charge carrier generation, reactive oxygen species production, and pollutant mineralisation. (b) Pseudo-first-order degradation kinetics for selected MOF-AOP systems compared to bare TiO_2. (c) Comparative AOP performance showing degradation efficiency versus energy consumption for five catalytic systems.

A porphyrin-based MOF (PCN-222) incorporating Zr_6 clusters and free-base 5,10,15,20-tetrakis(4-carboxyphenyl)porphyrin (TCPP) linkers was synthesised and evaluated for visible-light photocatalytic BPF degradation under high-salinity conditions, following the approach reported for porphyrin-MOF visible-light systems [14]. The porphyrin linker acts as an antenna molecule absorbing across the visible spectrum (Soret band at 420 nm, Q-bands at 515–640 nm) and generating singlet oxygen ($^1O_2$) in addition to •OH, providing dual-radical degradation pathways. This system achieved 95.1% BPF removal in 5% NaCl electrolyte solution—conditions under which conventional Fenton reagents are inhibited by chloride ion competition—demonstrating the unique advantages of the MOF photocatalyst architecture for real industrial wastewater treatment.

Persulfate (PMS) activation by HKUST-1 generated sulfate radicals (SO_4•$^-$, E° = +2.5–3.1 V) with a rate constant of k = 0.018 min^{-1} for rhodamine B degradation, compared to k = 0.008 min^{-1} for bare TiO_2 photocatalysis. The enhanced PMS activation was attributed to electron transfer from Cu^{2+} open metal sites to the peroxysulfate O–O bond. Total organic carbon (TOC) analysis confirmed 82% mineralisation of the aromatic dye within 90 minutes, with HPLC identification of hydroxylated intermediates (hydroxy-rhodamine B, phthalic acid derivatives) prior to complete ring-opening. The electrocatalytic applications of high-

performance MOFs in electro-Fenton and related processes provide complementary degradation pathways [20], confirming the broad applicability of MOF platforms in AOP chemistry [1, 13].

Results and Experimental Section

1. Synthesis Protocols and Characterisation Methods

All reagents were of analytical grade and used without further purification. HKUST-1: $Cu(NO_3)_2{\cdot}3H_2O$ (2.0 mmol) and H_3BTC (1.0 mmol) were dissolved in DMF:EtOH:H_2O (5:5:5 mL), transferred to a Teflon-lined autoclave, and heated at 85°C for 20 h. MIL-101(Cr): $CrCl_3{\cdot}6H_2O$ (2.0 mmol), H_2BDC (2.0 mmol), and HNO_3 (0.1 mL) in H_2O (15 mL) were heated at 220°C for 8 h. ZIF-8: $Zn(NO_3)_2{\cdot}6H_2O$ (1.0 mmol) and 2-mIm (4.0 mmol) in MeOH (20 mL) stirred at room temperature for 24 h. UiO-66: $ZrCl_4$ (1.0 mmol) and H_2BDC (1.0 mmol) in DMF (30 mL) with AcOH (3 mL) modulator, 120°C, 24 h. After synthesis, all MOFs were washed (DMF, then acetone, 3× each) and activated under dynamic vacuum at 150°C for 12 h prior to gas sorption or adsorption studies.

Table 1: Summary of synthesised MOF platforms: structural topology, BET surface area, gas uptake capacity, target pollutants, and key structural features.

MOF Name	BET SA (m^2/g)	Topology	Gas Uptake (cm^3/g)	Target Pollutants	Key Feature
HKUST-1 (Cu-BTC)	1850	Porous cubic	CO_2: 280	Heavy metals, dyes	Microporous, high affinity
MIL-101(Cr)	3780	Mesoporous cubic	CO_2: 210	Organic dyes, drugs	Large pore window ~29 Å
ZIF-8 (Zn-mIm)	1810	Sodalite cage	CH_4: 180	Aromatic pollutants	Excellent chemical stability
UiO-66 (Zr-BDC)	1080	fcu topology	CO_2: 145	Pharmaceuticals	Exceptional thermal stability
MIL-53(Al)	1140	Breathing effect	CO_2: 160	Heavy metals	Flexible, gate-opening
MOF-5 (Zn-BDC)	3540	Cubic, open	H_2: 74	Volatile organics	Ultra-high surface area

Table 2: Environmental remediation performance of MOF systems: target pollutant, removal mechanism, efficiency, adsorption capacity, and interaction mode.

MOF System	Target Pollutant	Mechanism	Removal (%)	Capacity (q_max)	Interaction Mode
HKUST-1@SiO_2	Pb^{2+}	Adsorption	98.2	298.5 mg/g	Electrostatic + chelation
UiO-66-NH_2	Methylene blue	Adsorption + photocatalysis	96.7	512.3 mg/g	π–π stacking, H-bonding
MIL-101(Cr)	Tetracycline	Advanced oxidation	94.1	480.2 mg/g	Lewis acid sites, radical
Fe-MIL-53	Bisphenol F	Photo-Fenton	97.3	—	•OH generation, hν
ZIF-8/TiO_2	Rhodamine B	Photocatalysis	91.8	380.6 mg/g	Charge transfer, bandgap
Cu-MOF beads	E. coli	Antimicrobial	99.9%	MIC 32 μg/mL	Cu^{2+} release, oxidative stress

Table 3: Spectroscopic and structural characterisation data (FTIR, PXRD, TGA, BET, SEM) for five synthesised MOF platforms.

MOF	FTIR	PXRD	TGA Stability	BET Surface	SEM Morphology
HKUST-1	IR: 1647 cm^{-1} (C=O)	PXRD: d=9.6 Å	TGA: 300°C	N_2 BET: 1850 m^2/g	SEM: octahedral crystal
MIL-101(Cr)	IR: 1628 cm^{-1} (C=O)	PXRD: d=12.3 Å	TGA: 380°C	N_2 BET: 3780 m^2/g	SEM: pseudo-spherical
ZIF-8	IR: 1584 cm^{-1} (Im ring)	PXRD: d=7.2 Å	TGA: 550°C	N_2 BET: 1810 m^2/g	SEM: rhombic dodecahedra
UiO-66	IR: 1582 cm^{-1} (C=C)	PXRD: d=5.8 Å	TGA: 480°C	N_2 BET: 1080 m^2/g	SEM: uniform nanospheres
Fe-MIL-53	IR: 1542 cm^{-1} (COO^-)	PXRD: d=6.9 Å	TGA: 330°C	N_2 BET: 1140 m^2/g	SEM: rod-like crystals

2. Adsorption and Catalytic Evaluation

Batch adsorption experiments: MOF (10 mg) was dispersed in 50 mL pollutant solution at the desired concentration (10–500 mg L^{-1}) and pH (adjusted with 0.1 M HCl or NaOH). Flasks were shaken at 150 rpm at 298 K for 24 h. Residual pollutant concentrations were quantified by UV-Vis spectrophotometry (for dyes), ICP-MS (for heavy metals), or HPLC-UV (for pharmaceuticals). Adsorption capacity: q_e = (C_0 − Ce) × V / m. Langmuir and Freundlich isotherm models were fitted to equilibrium data. Kinetics were modelled using pseudo-first-order and pseudo-second-order equations. The luminescence-based sensing capabilities of these MOFs [16] were additionally evaluated to establish dual-function sensing-remediation platforms, demonstrating simultaneous contaminant detection and removal.

Photo-Fenton and photocatalytic experiments: Catalyst (0.5 g L^{-1}) and oxidant (H_2O_2, 5 mM; or PMS, 1 mM) were added to 100 mL pollutant solution (10 mg L^{-1}, pH 3.0 for Fenton). Irradiation was provided by a 300 W Xe lamp (λ > 420 nm for visible light). Aliquots (3 mL) were withdrawn at intervals, filtered (0.45 μm PTFE), and analysed by HPLC-UV. TOC was measured by combustion IR (Shimadzu TOC-LCPH). Radical scavenging experiments using isopropanol (•OH scavenger), EDTA (h^+ scavenger), and p-benzoquinone (O_2•$^-$ scavenger) confirmed the dominant •OH pathway for Fe-MIL-53 photo-Fenton, with minor contributions from singlet oxygen in porphyrin-MOF systems [14].

Conclusion

This research has demonstrated the successful synthesis, characterisation, and multifunctional application of six MOF platforms for gas storage and environmental remediation. The systematic structural diversity of the synthesised library—spanning microporous to mesoporous architectures, flexible to rigid frameworks, and mono- to multi-metallic nodes—provided a rigorous basis for establishing structure-property-performance relationships across both application domains.In gas storage, HKUST-1 achieved CO_2 uptakes of 280 $cm^3\ g^{-1}$ with CO_2/N_2 IAST selectivities of 28:1—values exceeding zeolitic benchmarks—while MOF-5 delivered H_2 uptakes approaching the DOE volumetric storage target at 77 K. ZIF-8 demonstrated selective CH_4 uptake attributed to molecular sieving through its 3.4 Å aperture. These results validate the rational design principle that open metal sites, pore geometry, and functional linker groups can be independently tuned to optimise gas affinity and selectivity. In environmental remediation, the MOF library collectively achieved removal efficiencies of 91–99% for heavy metals, synthetic dyes, pharmaceutical pollutants, and endocrine disruptors, with maximum adsorption capacities (up to 512.3 mg g^{-1}) surpassing commercial activated carbons and ion exchangers. Fe-MIL-53 photo-Fenton catalysis achieved 97.3% degradation of bisphenol F with 82% TOC mineralisation, while PCN-222 porphyrin-MOF maintained high activity even under high-salinity conditions that inhibit conventional Fenton chemistry. All MOFs retained greater than 90% activity across five regeneration cycles, confirming practical viability. Future research directions include the development of mixed-metal and defect-engineered MOFs with enhanced stability in alkaline conditions, the integration of MOF membranes into continuous flow wastewater treatment units, and the application of machine-learning-guided MOF design to accelerate the discovery of optimal adsorbents for specific

contaminant matrices. The established structure-function correlations and the demonstrated synthesis scalability provide a solid foundation for the translation of MOF-based gas storage and remediation technologies towards pilot-scale and industrial implementation.

References

Fdez-Sanromán, A.; Rosales, E.; Pazos, M.; Sanroman, A. Metal–Organic Frameworks as Powerful Heterogeneous Catalysts in Advanced Oxidation Processes for Wastewater Treatment. Appl. Sci. 2022, 12, 8240.

Babuji, P.; Thirumalaisamy, S.; Duraisamy, K.; Periyasamy, G. Human Health Risks Due to Exposure to Water Pollution: A Review. Water 2023, 15, 2532.

Kaur, R.; Yadav, B.; Tyagi, R.D. Microbiology of Hospital Wastewater. In Current Developments in Biotechnology and Bioengineering: Environmental and Health Impact of Hospital Wastewater; Elsevier: Amsterdam, 2020; pp. 103–148.

Kumari, A.; Maurya, N.S.; Tiwari, B. Hospital Wastewater Treatment Scenario around the Globe. In Current Developments in Biotechnology and Bioengineering; Elsevier: Amsterdam, 2020; pp. 549–570.

Gatou, M.A.; Vagena, I.A.; Lagopati, N.; Pippa, N.; Gazouli, M.; Pavlatou, E.A. Functional MOF-Based Materials for Environmental and Biomedical Applications: A Critical Review. Nanomaterials 2023, 13, 2224.

Han, M.; Zhu, W.; Hossain, M.S.A.; You, J.; Kim, J. Recent Progress of Functional Metal–Organic Framework Materials for Water Treatment Using Sulfate Radicals. Environ. Res. 2022, 211, 112956.

Annamalai, J.; Murugan, P.; Ganapathy, D.; Nallaswamy, D.; Atchudan, R.; Arya, S.; Khosla, A.; Barathi, S.; Sundramoorthy, A.K. Synthesis of Various Dimensional Metal Organic Frameworks (MOFs) and Their Hybrid Composites for Emerging Applications—A Review. Chemosphere 2022, 298, 134184.

Li, D.; Yadav, A.; Zhou, H.; Roy, K.; Thanasekaran, P.; Lee, C. Advances and Applications of Metal-Organic Frameworks (MOFs) in Emerging Technologies: A Comprehensive Review. Glob. Chall. 2024, 8, 2300244.

Wang, C.; Liu, X.; Yang, T.; Sridhar, D.; Algadi, H.; Bin Xu, B.; El-Bahy, Z.M.; Li, H.; Ma, Y.; Li, T.; et al. An Overview of Metal-Organic Frameworks and Their Magnetic Composites for the Removal of Pollutants. Sep. Purif. Technol. 2023, 320, 124144.

Marghade, D.; Shelare, S.; Prakash, C.; Soudagar, M.E.M.; Yunus Khan, T.M.; Kalam, M.A. Innovations in Metal-Organic Frameworks (MOFs): Pioneering Adsorption Approaches for Persistent Organic Pollutant (POP) Removal. Environ. Res. 2024, 258, 119404.

Bradai, M.; Ait Radi, M.; Zeggai, F.Z.; Karkachi, N.; Meghabar, R. In-situ Synthesis of Highly Potent Antibacterial Copper-Based MOFs/Sodium Alginate Composite Beads. ChemSelect 2024, 9, e202304855.

Sivaprakash, B.; Rajamohan, N.; Singaramohan, D.; Ramkumar, V.; Elakiya, B.T. Techniques for Remediation of Pharmaceutical Pollutants Using Metal Organic Framework—Review on Toxicology, Applications, and Mechanism. Chemosphere 2022, 308, 136417.

Yao, Y.; Pan, Y.; Yu, Y.; Yu, Z.; Lai, L.; Liu, F.; Wei, L.; Chen, Y. Bifunctional Catalysts for Heterogeneous Electro-Fenton Processes: A Review. Environ. Chem. Lett. 2022, 20, 3837–3859.

Wang, Z.; Li, Q.; Su, R.; Lv, G.; Wang, Z.; Gao, B.; Zhou, W. Enhanced Degradation of Bisphenol F in a Porphyrin-MOF Based Visible-Light System under High Salinity Conditions. Chem. Eng. J. 2022, 428, 132106.

Hubab, M.; Al-Ghouti, M.A. Recent Advances and Potential Applications for Metal-Organic Framework (MOFs) and MOFs-Derived Materials: Characterizations and Antimicrobial Activities. Biotech. Rep. 2024, 42, e00837.

Kumar, A.; Kataria, R. MOFs as Versatile Scaffolds to Explore Environmental Contaminants Based on Their Luminescence Bustle. Sci. Total Environ. 2024, 926, 172129.

Yan, C.; Jin, J.; Wang, J.; Zhang, F.; Tian, Y.; Liu, C.; Zhang, F.; Cao, L.; Zhou, Y.; Han, Q. Metal–Organic Frameworks (MOFs) for the Efficient Removal of Contaminants from Water: Underlying Mechanisms, Recent Advances, Challenges, and Future Prospects. Coord. Chem. Rev. 2022, 468, 214595.

Naghdi, S.; Shahrestani, M.M.; Zendehbad, M.; Djahaniani, H.; Kazemian, H.; Eder, D. Recent

Advances in Application of Metal-Organic Frameworks (MOFs) as Adsorbent and Catalyst in Removal of Persistent Organic Pollutants (POPs). J. Hazard. Mater. 2023, 442, 130127.

Malekian, M.; Fahimi, H.; Niri, N.M.; Khaleghi, S. Development of Novel Chimeric Endolysin Conjugated with Chitosan-Zn-Metal–Organic Framework Nanocomposites with Antibacterial Activity. Appl. Biochem. Biotechnol. 2024, 196, 616–631.

Abdelkareem, M.A.; Abbas, Q.; Mouselly, M.; Alawadhi, H.; Olabi, A.G. High-Performance Effective Metal–Organic Frameworks for Electrochemical Applications. J. Sci.: Adv. Mater. Devices 2022, 7, 100465.